Multiphoton excitation and ionization of atomic cesium with a tunable dye laser*

D. Popescu
Institute of Physics of Bucharest, Bucharest, Romania

C. B. Collins and B. W. Johnson
The University of Texas at Dallas, Dallas, Texas 75230

Iovitzu Popescu
University of Bucharest, Bucharest, Romania

(Received 16 April 1973)

The two-photon excitation and three-photon ionization of atomic cesium is investigated over the 6550–6950-Å wavelength region with a tunable-dye-laser source having a 0.06–0.08-Å linewidth and a space-charge ionization detector sensitive to a few ions per second. An on-line data-acquisition computer provides significant signal-to-noise recovery. The resulting dispersion curve for photoionization is interpreted in terms of the two-photon transitions from the ground $6\,^2S_{1/2}$ level to resonant $n\,^2D$ and $n\,^2S$ intermediate states, and represents, to the authors' knowledge, the first such two-photon absorption spectrum of Cs. Transitions from $n=9$ to 13 have been recorded for the $6\,^2S_{1/2}-n\,^2D_{5/2,3/2}$ series and from $n=11$ to 14 for the $6\,^2S_{1/2}-n\,^2S_{1/2}$ series.

I. INTRODUCTION

Because the wavelengths of high-power lasers suitable for multiphoton ionization have been relatively fixed, tests of theory[1,2] have generally concerned the dependence of ionization yield on laser intensity rather than on wavelength. Recently the two-, three-, and four-photon ionization of atomic cesium has received particular attention at the 10 600- and 5300-Å Nd[3,4] and 6940-Å ruby laser[5,6] wavelengths. Results have been mixed with the latter being generally in better agreement with expectations than the former. The importance of resonant intermediate states is clearly indicated by theory, and the most recent experiments[7,8] which have achieved a limited range of wavelength tuning have shown considerable structure, often from molecular intermediate states not included in calculations.

The significant features to be expected in such a dispersion curve of multiphoton ionization can be readily appreciated. For cesium in the appropriate dipole approximation,[1] the three-photon ionization strength for ground-state atoms consists of sums over ground g and continuum state K degeneracies of terms of the form

$$S_{gK} \propto \left| \sum_i \sum_j \langle K|z|l_j\rangle \frac{\langle l_j|z|p_i\rangle}{E_j - E_0 - 2h\nu} \frac{\langle p_i|z|s\rangle}{E_i - E_0 - h\nu} \right|^2, \tag{1}$$

where the matrix elements are the usual dipole values and summations are implied over intermediate-state quantum numbers not explicitly expressed. The value of l can be either s or d in accordance with dipole selection rules and both must be included in the sum over index j.

It can be seen that the dispersion curve should be dominated by three effects, single-photon resonances, double-photon resonances, and accidental nodes resulting from cancellations in the sums. The first can result from a zero in the denominator of the term connecting the ground state with the first intermediate state, necessarily p in the dipole approximation,

$$T_1(p_i, s) = \langle p_i|z|s\rangle/(E_i - E_0 - h\nu), \tag{2}$$

and would give ionization peaks at wavelengths corresponding to the single-photon, principal series $6\,^2S$-$n\,^2P$ in absorption. Of greater interest is the second term,

$$T_2(l_j, p_i) = \langle l_j|z|p_i\rangle/(E_j - E_0 - 2h\nu), \tag{3}$$

as it makes possible two-photon absorption spectroscopy. Zeros in the denominator of this term give the expectation of ionization peaks at wavelengths corresponding to twice that of the normally forbidden absorption series $6\,^2S_{1/2}-n\,^2S_{1/2}$ and $6\,^2S_{1/2}-n\,^2D_{3/2,5/2}$. The details of these features together with the accidental cancellation effects appear in published[1] dispersion curves calculated for two- and three-photon ionization of atomic cesium in the low-field limit in which Stark broadening of the levels does not occur for the field intensities in the laser focus.

This paper reports observations of the three-photon ionization of atomic cesium as a continuous

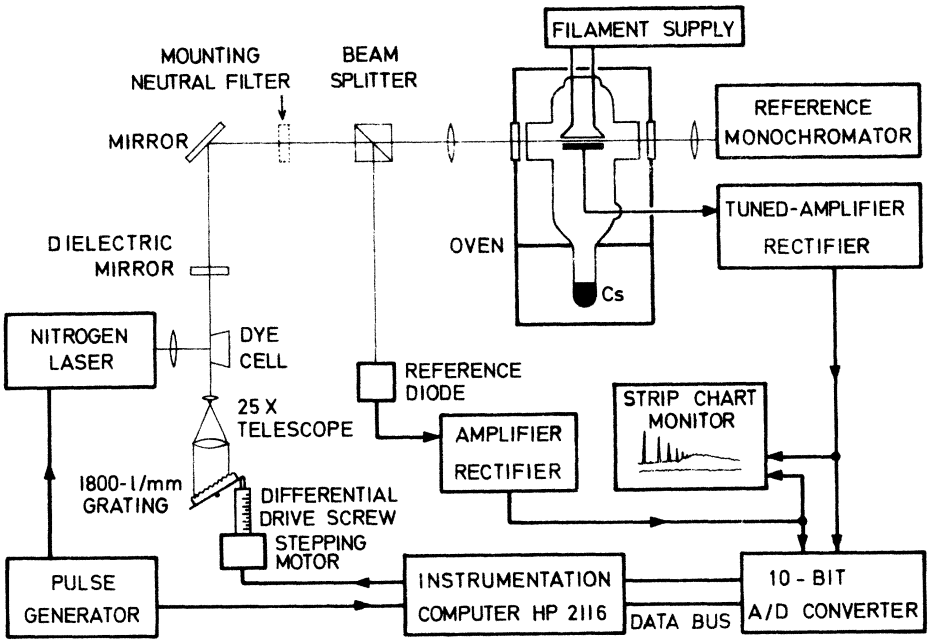

FIG. 1. Schematic representation of the arrangement of tunable dye laser, cesium absorption cell with included detector diode, and data-acquisition electronics used in these experiments.

function of laser wavelength and presents, to the authors' knowledge, the first such two-photon absorption spectrum of atomic cesium. The $6\,^2S_{1/2} - n\,^2D_{5/2,\,3/2}$ and $6\,^2S_{1/2} - n\,^2S_{1/2}$ series were obtained from $n = 9$ to 13 and $n = 11$ to 14, respectively, and shown to be the significant resonant intermediate states for three-photon ionization at those wavelengths. In a sense, the work reported here represents a generalization of the ruby-laser experiment in which the principal intermediate state has been reported[6,9] to be the $9\,^2D_{3/2}$ level broadened and shifted into resonance by the electric fields at the laser focus. Moreover, this work shows the examination of two-photon absorption spectra now to be as readily instrumented as conventional single-photon spectroscopy.

II. EXPERIMENTAL METHOD

Figure 1 shows the experimental arrangement used to obtain the multiphoton ionization spectra reported here. It consisted of a pulsed dye laser to produce the probing intensity, a cesium absorption cell containing a space-charge detector, and electronics suitable for synchronous detection and interfaced to an on-line instrumentation computer. Detail of the tunable dye laser is seen in the figure. Used with an 1800-lines/mm diffraction grating, a 25× beam-expanding telescope in the optical cavity gave a linewidth of 0.06–0.08 Å over the 6550–6950-Å tuning range used in these experiments. Stability of the wavelength from pulse to pulse was sufficient to insure indetectable broadening of the pattern when integrated over 50 successive laser pulses in an analyzing Fabry-Perot having 1-Å free spectral range. The particular dye used was a mixture of Cresyl Violet, Rhodamine 6G, and HCl and was pumped with a pulsed nitrogen laser delivering about 50-kW peak power. Pulse widths were of the order of 15 nsec and repetition rates were 8 sec^{-1} as limited by drift times for ions within the space-charge detector. The wavelength drive consisted of a differential screw which rotated the grating as shown in the figure. A stepping motor interfaced to the data-acquisition computer served to advance the wavelengths in 0.03-Å steps.

The output laser beam was focused into the cesium absorption cell containing the diode detector, a 0.15-mm tungsten wire filament and a silver-disk anode, both activated with cesium and separated by 1.5 mm. The exact position of the focal volume within the diode structure was not found to be particularly critical provided the diode elements themselves were not directly illuminated by the laser. It was only required that the positive ions, either directly or indirectly produced from the absorption process, be able to diffuse or drift into the space-charge cloud surrounding the heated filament. Then, by partially neutralizing the negative charge for the relatively longer time the ions spent traversing the space-charge region, they provided for the release from the region of the order of 10^5 to 10^6 electrons per ion.[10,11] Satisfactory signal-to-noise ratios in the resulting diode current were found to be optimized for a

working pressure corresponding to a saturated vapor of 490 °K. Under these conditions, the sensitivity to both atomic and molecular ions is expected to be roughly equal.[11] Number densities of neutral cesium atoms and molecules were of the order of 3.1×10^{15} cm^{-3} and 7.8×10^{12} cm^{-3}, respectively. Optimal filament temperatures were around 1100 °K.

As the laser output was not of constant intensity either as a function of time or wavelength, it was necessary to simultaneously record both it and the diode output current for each laser pulse. This was accomplished as shown in Fig. 1 with a 10-bit analog-to-digital conversion system directly interfaced to the instrumentation computer. A time-average signal for each wavelength step was obtained by successive sampling for a sequence of laser pulses under software control. Depending upon laser wavelength and cavity alignment, from 20 to 50 pulses per wavelength step were found to be adequate to ensure good reproducibility of the resulting averages.

III. RESULTS AND ANALYSIS

Useable laser intensities spanned the wavelength range from 6550 to 6950 Å, which had been expected to contain many of the two-photon resonances of interest to this work. The energy-level diagram of Fig. 2 serves to relate these wavelengths to the transitions to intermediate states of the cesium atom. The range of photon energies covered by the experiment is indicated by the blocks near the heads of arrows representing transitions to the intermediate states. The lower shaded block bounds the energy of the transition to the first, nonresonant, intermediate P state and the upper blocks, the energy of the second, two-photon transition. Since the latter contains both $n\,^2D$ and $n\,^2S$ levels, resonances would be expected at those appropriate wavelengths. Conversely, as the extent of the lower shaded rectangle is of the order of its separation from the nearest, $6\,^2P$, level, little modulation of the dispersion curve would be expected to result from the variation of

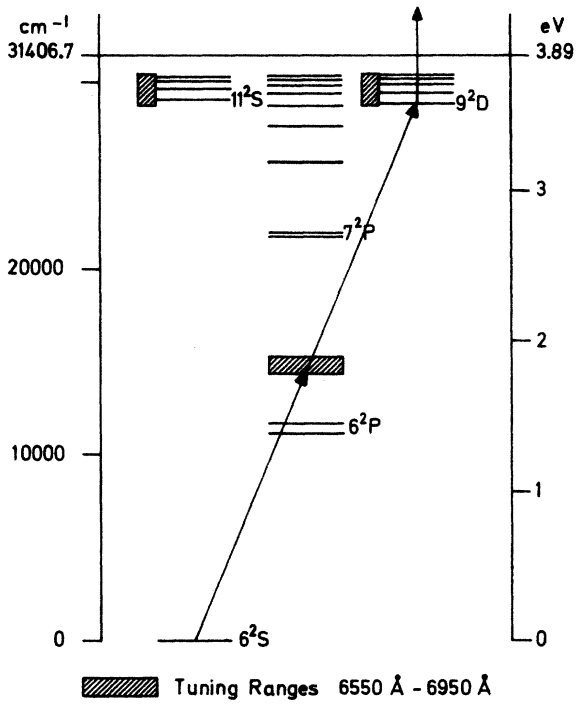

FIG. 2. Energy-level diagram of the states of atomic Cs relevant to three-photon photoionization over the 6550–6950-Å range of wavelengths covered in this experiment. The corresponding range of photon energies is indicated by the shaded rectangular blocks, the lower rectangle bounding energies of transitions to the first, nonresonant, intermediate P state, and the upper rectangles bounding energies of the second, two-photon transition.

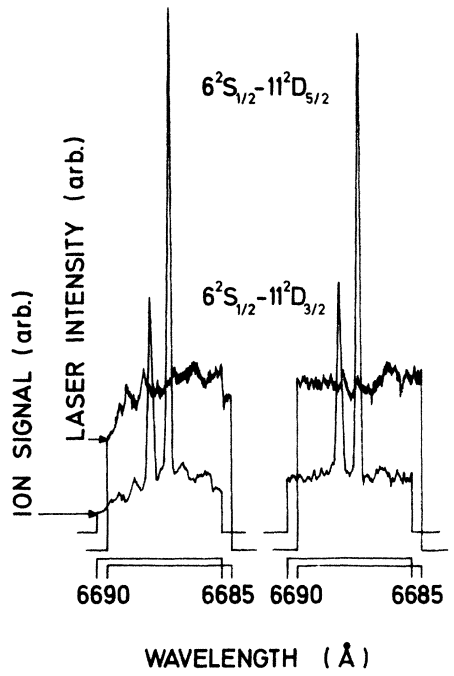

FIG. 3. Direct recording of the detected ion current (lower curve) and input laser intensity (upper curve) as functions of wavelength for the 5-Å interval around 6687 Å. Sharp minima at the beginning and end of each segment record the dark current from detectors and electronics, and two pair of data are shown to indicate the degree of reproducibility of the basic data prior to the use of the digital, signal recovery techniques. The offset in wavelengths between ion current and laser intensity is an artifact of the two-pen recorder.

photon energy with respect to the energy of the transition to the nearest, nonresonant, P state. At least for the $6\,^2P$ term, from Eq. (2) we would expect

$$dT_1(6\,^2P, s)/T_1(6\,^2P, s) = -d(h\nu)/(E_i - E_0 - h\nu), \tag{4}$$

indicating less than 50% variation of this term over the entire tuning range. Variation in the other T_1 terms would be even less, so that, except for the possibility of accidental cancellations, the multiphoton ionization spectrum over this wavelength region should correspond to that for two-photon absorption.

Figure 3 presents the unprocessed data for both detected ion current and input laser intensity as functions of wavelength for the 5-Å interval around 6687 Å and tends to confirm the theoretical expectations. The photon energies scanned correspond to those near the two-photon resonances $T_2(11\,^2D, p_i)$, corresponding to transitions from the ground to the $11\,^2D_{3/2,5/2}$ levels. Two pairs of measurements of the same region are shown to illustrate the absolute level of noise and nonreproducibility of the laser output. These particular records were taken from the dual-channel strip-chart recorded used to monitor the experiment and, therefore, had not benefitted from the real-time normalization and averaging available from the digital-data-acquisition system. Nevertheless, the $11\,^2D$ doublet is clearly identifiable and reproducible even in the raw data.

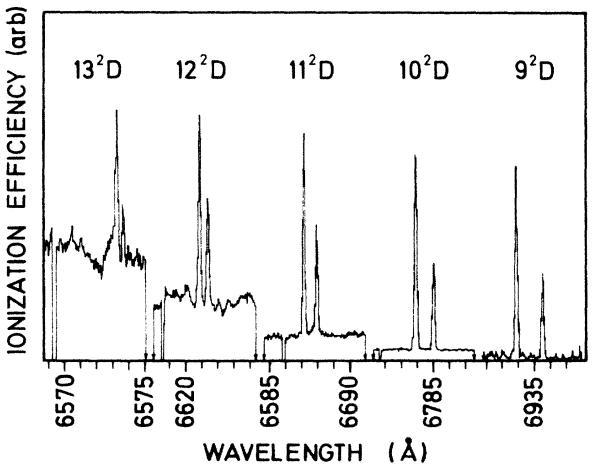

FIG. 4. Photoionization efficiency as a function of laser wavelength for five wavelength intervals containing components of the $6\,^2S_{1/2} \rightarrow n\,^2D_{5/2,3/2}$ two-photon absorption series. The ratio of signal-less-dark-current to the square of the laser intensity is shown in arbitrary units. The value of n appropriate to each interval is indicated. The wavelength scale is marked in 1-Å increments from the calibration wavelength explicitly indentified within each segment and is not continuous between segments.

Figure 4 presents the photoionization signal recorded in the digital channels as a function of laser wavelength. Five wavelength segments are shown which correspond to two-photon absorptions of the $n = 9$–14 members of the $6\,^2S_{1/2} \rightarrow n\,^2D_{5/2,3/2}$ spectral series. The diode dark current seen at the beginning and end of the 5-Å regions in Fig. 3 has been subtracted and the data scaled by the square of the simultaneously measured laser intensity. The apparent width of the atomic lines seen in the figure is characteristic of the laser linewidth as measured interferometrically. In these spectrum segments, the sharp minima were artificially introduced to provide a calibration of zero-signal and, in fact, no evidence of a spurious cancellation was found over the wavelength region examined. In a similar sense, it should be noted that the background signal present in some segments is most probably attributable not to the summation of the nonresonant terms of Eq. (1), but rather to the masking of the two-photon atomic lines by components of the two-photon, photoionization of Cs_2 through transitions to the resonant intermediate C states of Cs_2. Such a process would be described in a manner analogous to (1), but with only sums over the continuum and T_1 terms. The detail of the background to the atomic lines of Fig. 4 does not result from noise but from the single-photon resonances in the T_1 term for the two-photon ionization of Cs_2 corresponding to the $(X^1\Sigma_g^+ \rightarrow C)$ single-photon absorption band. A recent[8] examination of this background in the 6200–6600-Å region has shown it to reproduce in detail the structure of the transitions between various vibrational levels of the molecular states involved. Being a two-photon process, it was theoretically expected and experimentally confirmed[8] that the ionization signal from the molecular background had a square-law dependence on laser intensity. These prior results provided the basis for scaling the ionization signal by the inverse square of the laser intensity in the present work.

It can be seen from Fig. 4 that both the $9\,^2D_{5/2}$ and $9\,^2D_{3/2}$ levels are clearly isolated in the 6936-Å region of the two-photon absorption spectrum. This suggests that the prior ruby-laser experiments should be most directly comparable to theory as developed to include only potentially resonant intermediate atomic states. More generally, it can be noted that the wavelengths for which one of the $9\,^2D_{5/2}$, $9\,^2D_{3/2}$, $10\,^2D_{5/2}$, and $10\,^2D_{3/2}$ levels serves as the principal intermediate state nearest in energy to $2h\nu$ in excess of that of the $6\,^2S_{1/2}$ state should have intensity-dependent ionization yields most in agreement with theory.

Conversely, it can be seen that transitions to states of higher energy lie in regions of the two-photon spectrum containing molecular structures.

It is interesting to note that, as expected from the fact that the ionization strength for the $n\,^2D_{5/2,3/2}$ doublets depends on sums over products of $T_2(n\,^2D, p_i)$ and $T_1(p_i, 6\,^2S)$ terms, where p_i represents the set of all quantum numbers belonging to possible intermediate, nonresonant P states, the intensity ratio of the doublets differs from the corresponding 3:2 ratio[12] for the single-photon excitation of the quadrupole transition at twice the frequency.

Figure 5 shows the similar two-photon absorption spectrum for the $n = 11-14$ members of the $6\,^2S_{1/2} \rightarrow n\,^2S_{1/2}$ series. As in the case of the S-D series, the longer wavelength transitions are clearly isolated, while the shorter lie in congested regions of the spectrum. The $6\,^2S_{1/2} \rightarrow 14\,^2S_{1/2}$ line at 6599.3 Å shows the typical masking of the atomic lines by the molecular components, which prevented any further extension of the atomic series to shorter wavelengths. This masking of atomic lines with increasing principal quantum number n is accentuated by a very rapid decrease of the two-photon absorption probability with increasing n.

Evidently, the study of the dependence of ionization yield upon laser intensity can have meaning in terms of the simple atomic theory only for the longer wavelengths. Because the intensity of the dye-laser system lay in the region of a few kilowatts, examination of this dependence was limited to the wavelengths of resonance with one of the lines shown in Figs. 4 and 5. The $6\,^2S_{1/2} \rightarrow 10\,^2D_{5/2}$ transition at 6784.0 Å was selected as a compromise between limitations on the efficiency of the dye fluorescence and the necessity to avoid molecular components. As can be seen in the resulting data presented in Fig. 6, only at the highest laser intensity that could be arranged did the use of neutral-density filters show agreement with the third-order dependence of ionization yield on laser intensity expected for the three-photon ionization of cesium in the absence of saturation of the intermediate transitions. At the lower intensities, the dependence can be seen to suggest a lower order not in disagreement with a value of two. The quadratic dependence of the molecular background has been included for comparison. The $9\,^2D$ levels could not be observed at intensities sufficiently great to show other than the low-intensity, second-order dependence. The resulting variation of the dependence of ionization yield on laser intensity suggests the competition of two channels for the final step of ionization. In addition to the direct three-photon ionization

$$\mathrm{Cs} + (3h\nu) \rightarrow \mathrm{Cs}^+ + e, \tag{5}$$

through the resonant $n\,^2D$ and $n\,^2S$ levels, the collisional ionization of the intermediate state formed by the two-photon absorption

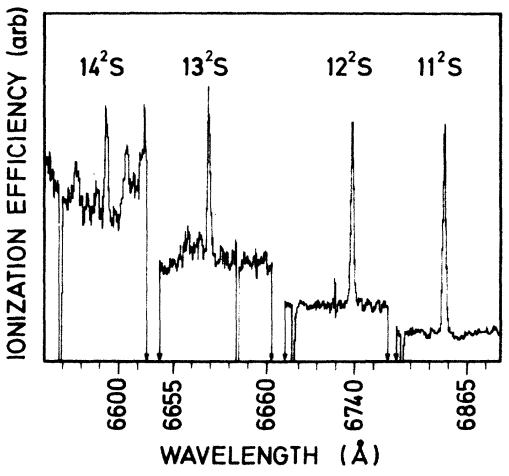

FIG. 5. Photoionization efficiency as a function of laser wavelength for four wavelength intervals containing components of the $6\,^2S_{1/2} \rightarrow n\,^2S_{1/2}$ two-photon absorption series. The ratio of signal-less-dark-current to the square of the laser intensity is shown in arbitrary units. The value of n appropriate to each interval is indicated. The wavelength scale is marked in 1-Å increments from the calibration wavelength explicitly identified within each segment and is not continuous between segments.

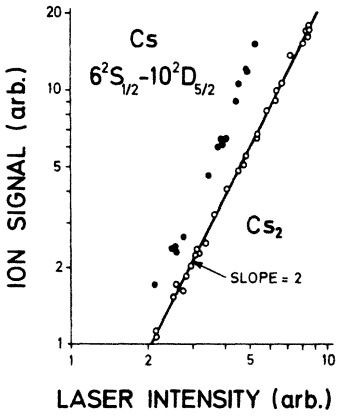

FIG. 6. Photoionization current less dark current as a function of laser intensity. ●: ion signals corresponding to the peak of two-photon absorption, $6\,^2S_{1/2} \rightarrow 10\,^2D_{5/2}$, at 6784.0 Å. The data plotted is the peak-detected ion current less baseline current seen in Fig. 4; this baseline is attributable to photoionization of Cs_2. ○: ion signals corresponding to the purely molecular two-photon ionization of Cs_2 presented for comparison.

$$Cs + (2h\nu) \rightarrow Cs^*(n\,^2D, n\,^2S), \quad (6)$$

is probable by either associative ionization if $n \leq 12$:

$$Cs^* + Cs \rightarrow Cs_2^+ + e, \quad (7)$$

or by molecular association followed by dissociative attachment, as suggested by Lee and Mahan[13] when $n > 12$:

$$Cs^* + Cs \rightarrow Cs_2^* \rightarrow Cs^+ + Cs^-. \quad (8)$$

While some estimates of the rate coefficient for associative ionization (7) have been so large as to suggest a unit probability for ionization of any resulting excited states under the conditions of this experiment, quantitative measurement[10] of f values and ionization probabilities as functions of increasing n have reported that the latter values do not reach 10^{-2}, at least for $n\,^2P$ levels, until $n \geq 12$. Thus it appears unlikely the ionization channel for S and D levels should be saturated by either (7) or (8) for the lower principal quantum numbers and reaction (6) followed by either (7) or (8) should yield a second-order dependence of ionization on laser intensity, while (5) should give a cubic term in the absence of saturation. The data of Fig. 6 suggests the competition between the two channels favors collisional processes at low intensities and radiative at the higher values, as would be expected.

It appears, then, that the two-photon absorption spectrum is shown to be a useful tool for the understanding of multiphoton ionization in cesium. Furthermore, because of the highly resonant nature of such excitations through intermediate states, the availability of tunable dye lasers of high spectral density now makes multiphoton absorption spectra as readily obtainable as conventional single-photon spectra.

---

*Work conducted as part of the U. S.-Romania Cooperative Program in Science and Technology in association between the University of Texas at Dallas and the Institute of Physics of Bucharest. Financial support was provided in part by the U. S. National Science Foundation under Grant No. GF443 and in part by the Romanian Comitetul de Stat pentru Energia Nucleara and the Consiliul National pentru Stiinta Si Tehnologie.

[1]H. B. Bebb, Phys. Rev. 153, 23 (1967).
[2]G. S. Voronev, Zh. Eksp. Teor. Fiz. 51, 1496 (1966) [Sov. Phys.—JETP 24, 1009 (1967)].
[3]B. Held, G. Mainfray, C. Manus, and J. Morellec, Phys. Lett. A 35, 267 (1971).
[4]B. Held, G. Mainfray, C. Manus, and J. Morellec, Phys. Rev. Lett. 28, 130 (1972).
[5]R. A. Fox, R. M. Kogan, and E. J. Robinson, Phys. Rev. Lett. 26, 1416 (1972).
[6]R. G. Evans and P. G. Thonemann, Phys. Lett. A 39, 133 (1972).
[7]B. Held, G. Mainfray, C. Manus, J. Morellec, and F. Sanchez, Phys. Rev. Lett. 30, 423 (1972).
[8]C. B. Collins, B. W. Johnson, D. Popescu, G. Musa, M. L. Pascu, and Iovitzu Popescu, Phys. Rev. A 8, 2197 (1973).
[9]I. D. Abella, Phys. Rev. Lett. 9, 453 (1962).
[10]D. Popescu, M. L. Pascu, C. B. Collins, B. W. Johnson, and I. Popescu, Phys. Rev. A 8, 1666 (1973).
[11]G. V. Marr and S. R. Wherrett, J. Phys. B 5, (1972).
[12]E. U. Condon and G. H. Shortley, *The Theory of Atomic Spectra* (Cambridge U. P., New York, 1967), p. 254.
[13]Y. T. Lee and B. H. Mahan, J. Chem. Phys. 42, 2893 (1965).